

1 **Azimuthal transverse single-spin asymmetries of**  
2 **inclusive jets and hadrons within jets from polarized**  
3  **$pp$  collisions at  $\sqrt{s} = 510$  GeV**

---

4 **Yixin Zhang<sup>a,\*</sup>, for the STAR Collaboration**

5 <sup>a</sup>*Institute of Frontier and Interdisciplinary Science & Key Laboratory of Particle Physics and Particle*  
6 *Irradiation (Ministry of Education), Shandong University, Qingdao, Shandong, 26623 China*

7 *E-mail: [yx\\_zhang@mail.sdu.edu.cn](mailto:yx_zhang@mail.sdu.edu.cn)*

The study of the origin of transverse single-spin asymmetries has triggered the development of the twist-3 formalism and the transverse-momentum-dependent parton distribution functions (TMDs). Measurements of the azimuthal distribution of identified hadrons within a jet in transversely polarized hadronic interactions provide opportunities to study TMD physics, such as the Collins effect which involves the quark transversity and the Collins fragmentation functions. STAR has reported measurements of the Collins asymmetries from jet +  $\pi^\pm$  production in transversely polarized  $pp$  collisions at a center-of-mass energy of  $\sqrt{s} = 500$  GeV based on data taken in 2011 with an integrated luminosity of  $23 \text{ pb}^{-1}$ . Additionally, an extensive measurement of azimuthal transverse single-spin asymmetries of inclusive jets and hadrons within jets from transversely polarized  $pp$  collisions at  $\sqrt{s} = 200$  GeV was performed using data from 2012 and 2015. In 2017, STAR collected a significantly larger  $pp$  dataset with an integrated luminosity of  $320 \text{ pb}^{-1}$  at  $\sqrt{s} = 510$  GeV, which will further improve the precision of the transverse single-spin asymmetry measurements, especially in the high jet transverse momentum region. In this contribution, we report the preliminary results of azimuthal transverse single-spin asymmetries for inclusive jets and charged pions within jets from transversely polarized  $pp$  collisions at  $\sqrt{s} = 510$  GeV.

*25th International Spin Physics Symposium (SPIN 2023)*  
*24-29 September 2023*  
*Durham, NC, USA*

---

\*Speaker

## 9 1. Introduction

10 Anomalous large transverse single-spin asymmetry,  $A_N$ , for inclusive hadrons has been  
11 observed in transversely polarized hadron-hadron collisions at different energies [1]. Leading  
12 order perturbative quantum chromodynamics (pQCD) cannot describe such large asymmetry [2].  
13 Presently, there are two QCD frameworks developed to explain the observed asymmetries: the high  
14 twist and transverse-momentum-dependent (TMD) formalisms.

15 The twist-3 formalism utilizes the initial-state and final-state multi-parton correlators within  
16 collinear pQCD framework, with a single hard scale,  $Q$ , which is much larger than  $\Lambda_{QCD}$  [3, 4].  
17 Unlike twist-3, the TMD formalism utilizes the leading-twist framework of pQCD beyond the  
18 collinear assumption, with a large scale  $Q$  and a soft scale such as the transverse momentum,  $p_T$ .  
19 It requires correlations between spin polarization and intrinsic transverse momentum either in the  
20 initial state or final state. The Sivers effect and Collins effect are two typical examples of TMD  
21 mechanisms. The initial-state Sivers effect requires a correlation between the nucleon spin and the  
22 intrinsic transverse momentum,  $k_T$ , of the parton inside the nucleon [5]. On the other hand, the  
23 final-state Collins effect requires a correlation between the quark spin and the transverse momentum  
24 of a hadron relative to the quark direction [6]. In semi-inclusive deep inelastic scattering (SIDIS)  
25 and hadronic interaction, the Collins effect is generated by a nonzero transversity coupled to the  
26 Collins fragmentation function [7, 8].

27 The issue of whether TMD factorization holds or not in the context of transversely polarized  
28  $pp$  collisions is discussed in [9–14]. This can be verified by comparing the measured Collins  
29 asymmetry against theoretical predictions extracted from global analyses of  $e^+e^-$  annihilation and  
30 deep inelastic scattering (DIS) processes. Further insight into the potential energy dependence of  
31 the Collins effect can be gained by comparing Collins asymmetry at different collision energies.

32 Previously, STAR has measured the Sivers asymmetry of inclusive jets and Collins asymmetries  
33 of hadron in jets in  $pp$  collisions at  $\sqrt{s} = 500$  GeV with an integrated luminosity of  $23 \text{ pb}^{-1}$  [15]  
34 and at  $\sqrt{s} = 200$  GeV with an integrated luminosity of  $74 \text{ pb}^{-1}$  [17]. In this contribution, we report  
35 new preliminary results on Sivers asymmetry of jets and charged pion Collins asymmetry with a  
36 much larger data sample of  $320 \text{ pb}^{-1}$  at  $\sqrt{s} = 510$  GeV.

## 37 2. Data Analysis

38 The Relativistic Heavy Ion Collider (RHIC) is currently the world's only facility capable of  
39 colliding high energy beams of polarized protons. Transversely polarized proton-proton collision  
40 data samples have been taken in recent years at STAR. The dataset used in this analysis was recorded  
41 in 2017 at  $\sqrt{s} = 510$  GeV and the proton beam polarization is about 55%. The STAR detectors  
42 used in this analysis are the Time Projection Chamber (TPC) [18], Time-of-Flight (TOF) [19] and  
43 Electromagnetic Calorimeter (EMC) [20, 21]. The TPC provides charged particle tracking and  
44 TOF measures the particle flight time. Both of which provide particle identification. The Barrel  
45 and endcap EMC measure the energy deposits from photons, electrons and  $\pi^0$ .

46 Jets and hadrons within jets are used to probe the transverse single-spin asymmetry since  
47 inclusive hadrons are incapable of discriminating between the Sivers and Collins effects. Jet  
48 reconstruction utilizes the anti- $k_T$  algorithm with parameter  $R = 0.5$ , which follows previous jet

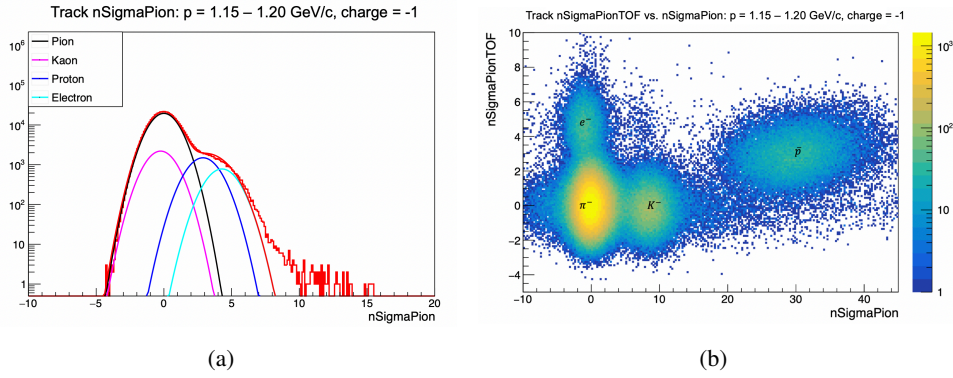


**Figure 1:** The particle rich region for TOF unmatched (a) and matched (b) using tracks with momentum range of (1.15, 1.20 GeV/c) as an example.

49 analysis [15]. Inputs to the jet finder contain charged tracks from the TPC and EMC tower energies.  
 50 The off-axis cone method [16] is used to estimate the underlying event contribution. The hadron  
 51 within jet asymmetries are measured with identified charged particles. Particle identification relies  
 52 on energy loss ( $dE/dx$ ) obtained through the TPC and the particle's flight time obtained through  
 53 the TOF. The energy loss, denoted as  $dE/dx$ , can be represented as  $n\sigma_{dE/dx}$  and is expressed by  
 54 the following formula:

$$n\sigma_{dE/dx} = \frac{1}{\sigma_{\text{exp}}} \ln \left( \frac{dE/dx_{\text{obs}}}{dE/dx_{\text{cal}}} \right), \quad (1)$$

55 where  $dE/dx_{\text{obs}}$  and  $dE/dx_{\text{cal}}$  are the measured energy loss of charged tracks and the expected  
 56 energy loss based on the Bichsel formalism, respectively, and  $\sigma_{\text{exp}}$  is the TPC  $dE/dx$  resolution.  
 57 Similarly  $n\sigma_{TOF}$ :

$$n\sigma_{TOF} = \frac{TOF_{\text{meas}} - \frac{L}{c\beta(p)}}{\sigma_{\text{eff}}}, \quad (2)$$

58 where  $TOF_{\text{meas}}$  is the measured flight time,  $L/c\beta$  is the expected value of the flight time cal-  
 59 culated through the path length( $L$ ), the speed of light( $c$ ), and the inverse velocity( $1/\beta$ ), where  
 60  $\beta = 1/\sqrt{1 + m^2/p^2}$  and  $p$  is the momentum of the particle.  $\sigma_{\text{eff}}$  accounts for the time resolution  
 61 of the TOF detector. In Fig. 1, each particle species rich sample is identified using the TPC and  
 62 TOF. Figure 1(a) corresponds to tracks without TOF match, where a multi-Gaussian is utilized to  
 63 fit the  $n\sigma_{dE/dx}$  distribution. Figure 1(b) corresponds to tracks matched with a TOF hit, where a  
 64 two-dimensional multi-Gaussian is used to fit the 2D  $n\sigma_{dE/dx}$  vs.  $n\sigma_{TOF}$  distribution. The raw  
 65 asymmetries and particle fractions can be extracted in each particle rich region, and then the pure  
 66 asymmetries can be calculated through the Moore-Penrose matrix inversion, which is similar to  
 67 [17].

68 For  $\pi^\pm$  within jets in  $pp$  collisions, the spin-dependent cross section can be expressed as [24]:

$$\begin{aligned}
 & \frac{d\sigma^\uparrow(\phi_S, \phi_H) - d\sigma^\downarrow(\phi_S, \phi_H)}{d\sigma^\uparrow(\phi_S, \phi_H) + d\sigma^\downarrow(\phi_S, \phi_H)} \\
 & \propto A_{UT}^{\sin(\phi_S)} \sin(\phi_S) \\
 & + A_{UT}^{\sin(\phi_S - \phi_H)} \sin(\phi_S - \phi_H) \\
 & + A_{UT}^{\sin(\phi_S - 2\phi_H)} \sin(\phi_S - 2\phi_H) \\
 & + A_{UT}^{\sin(\phi_S + \phi_H)} \sin(\phi_S + \phi_H) \\
 & + A_{UT}^{\sin(\phi_S + 2\phi_H)} \sin(\phi_S + 2\phi_H),
 \end{aligned} \tag{3}$$

69 where  $\phi_S$  is the angle between the proton spin direction and the reaction plane,  $\phi_H$  is the angle of the  
 70  $\pi^\pm$  momentum transverse to the jet axis relative to the reaction plane. Different angle modulations  
 71 are related to different effects. The first term,  $\sin(\phi_S)$ , is related to Sivers effect, and the second term,  
 72  $\sin(\phi_S - \phi_H)$ , is related to the Collins effect. The inclusive jet asymmetry is related to the twist-3  
 73 distribution of the  $k_T$ -integrated Sivers function [27]. The  $A_{UT}^{\sin(\phi_S)}$  for jets containing a  $\pi^+$  or  $\pi^-$   
 74 with a longitudinal momentum fraction  $z > 0.3$  can enhance the  $u$  and  $d$  quark fractions [17, 28, 29].  
 75 At low jet  $p_T$ , the asymmetries are sensitive to gluonic subprocesses, and with increasing jet  $p_T$ ,  
 76 the asymmetries become sensitive to quark subprocesses.

77 For each modulation, the transverse single-spin asymmetry is extracted using the "cross-ratio"  
 78 method to cancel detector efficiency and spin-dependent luminosity:

$$A_N \sin(\phi) = \frac{1}{P} \cdot \frac{\sqrt{N^\uparrow(\phi)N^\downarrow(\phi + \pi)} - \sqrt{N^\downarrow(\phi)N^\uparrow(\phi + \pi)}}{\sqrt{N^\uparrow(\phi)N^\downarrow(\phi + \pi)} + \sqrt{N^\downarrow(\phi)N^\uparrow(\phi + \pi)}}, \tag{4}$$

79 where  $N^\uparrow$  and  $N^\downarrow$  are the jet or hadron in jet yields for a given spin state, and  $\phi$  is the corresponding  
 80 angle for the different modulations.

### 81 3. Results

82 The Sivers asymmetry of inclusive jets and jets that contain a charged pion with longitudinal  
 83 momentum fraction  $z > 0.3$  versus particle jet  $p_T$  is presented in Fig. 2. Both inclusive jets  
 84 asymmetry and  $\pi^\pm$ -tagged jet asymmetries are consistent with zero within uncertainties, which is  
 85 similar to previous STAR results in polarized  $pp$  collisions at  $\sqrt{s} = 200$  and  $\sqrt{s} = 500$  GeV [15, 17].

86 Figure 3 shows the Collins asymmetries for  $\pi^\pm$  within a jet as a function of particle jet  $p_T$   
 87 from  $pp$  collisions at  $\sqrt{s} = 510$  GeV at STAR taken in 2017. New results are consistent with  
 88 previous data [15], but with much better statistical precision. The asymmetries are positive for  $\pi^+$   
 89 and negative for  $\pi^-$  because  $\pi^+$  and  $\pi^-$  are mostly from favored fragmentation of  $u$  and  $d$  quark,  
 90 respectively. A global analyses of SIDIS and  $e^+e^-$  annihilation indicate that the  $u$  quark transversity  
 91 is positive, while the  $d$  quark transversity is negative. The Collins asymmetry only exists for quark  
 92 subprocesses because the gluon transversity distribution is expressed by the amplitude of the gluon  
 93 helicity flip [22, 23]. Therefore, the gluon transversity does not exist for spin-1/2 nucleons due to  
 94 the helicity-conservation constraint. Thus, the asymmetries are small at low jet  $p_T$  and increase  
 95 with increasing jet  $p_T$  which is sensitive to gluon-quark subprocesses. Figure 4 shows a comparison  
 96 of the new Collins asymmetry at  $\sqrt{s} = 510$  GeV with the  $\sqrt{s} = 200$  GeV results as a function of jet

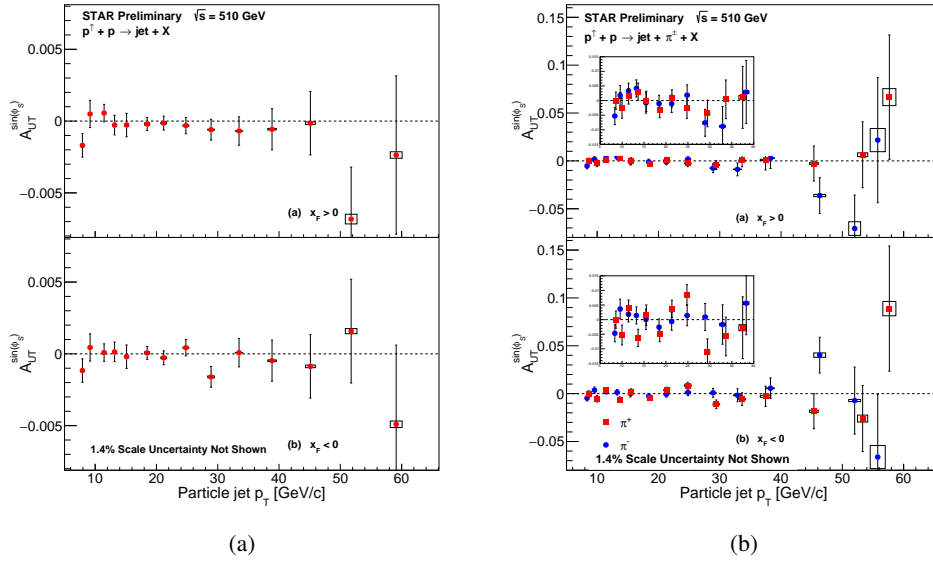


**Figure 2:** The Sivers asymmetries,  $A_{UT}^{\sin(\phi_S)}$ , of inclusive jets (a) and  $\pi^\pm$  tagged jets with  $z > 0.3$  (b). The top panels shows results for jets that scatter forward relative to the polarized beam ( $x_F > 0$ ), while the bottom panels shows jets that scatter backward to the polarized beam ( $x_F < 0$ ).

97  $x_T (= 2p_T/\sqrt{s})$ . These two results with different beam energies nicely align with the jet  $x_T$  scale,  
 98 indicating almost no energy dependence, which will provide important constraints on the scale  
 99 evolution.

100 Figures 5 and 6 show the Collins asymmetries as a function of the charged pion's longitudinal  
 101 momentum fraction,  $z$ , and the charged pion's transverse momentum relative to the jet axis,  $j_T$ ,  
 102 respectively in different jet  $p_T$  bins. These results provide more detailed constraints on the Collins  
 103 fragmentation function. Figure 7 shows the comparison of the new Collins asymmetries at  $\sqrt{s} =$   
 104 510 GeV with the  $\sqrt{s} = 200$  GeV results, as a function of  $j_T$  of the charged pion in different  $z$   
 105 bins. Once again, these asymmetries are in good agreement, further indicating Collins effect has  
 106 no energy dependence.

107 Figure 8 shows the Collins asymmetries at  $\sqrt{s} = 510/500$  GeV in comparison with three sets of  
 108 model calculations [14, 30], which are based on global analyses of SIDIS and  $e^+e^-$  results. Each  
 109 set assumes robust factorization and universality of the Collins function. The DMP+2013 [30]  
 110 and KPRY [14] predictions assume no TMD evolution while the KPRY-NLL [14] assumes TMD  
 111 evolution up to next-to-leading-logarithmic. Overall, the experimental measurements are consistent  
 112 with theoretical predictions within uncertainty, although the theoretical values are systematically  
 113 lower than the experimental results.

#### 114 4. Conclusion

115 In this contribution, we present the transverse single-spin asymmetries of jets and  $\pi^\pm$  within  
 116 jets in  $pp$  collisions at  $\sqrt{s} = 510$  GeV with STAR 2017 data, which has 14 times more statistics than  
 117 the previous measurement. The high precision Collins asymmetries for  $\pi^+$  and  $\pi^-$  results at  $\sqrt{s} =$

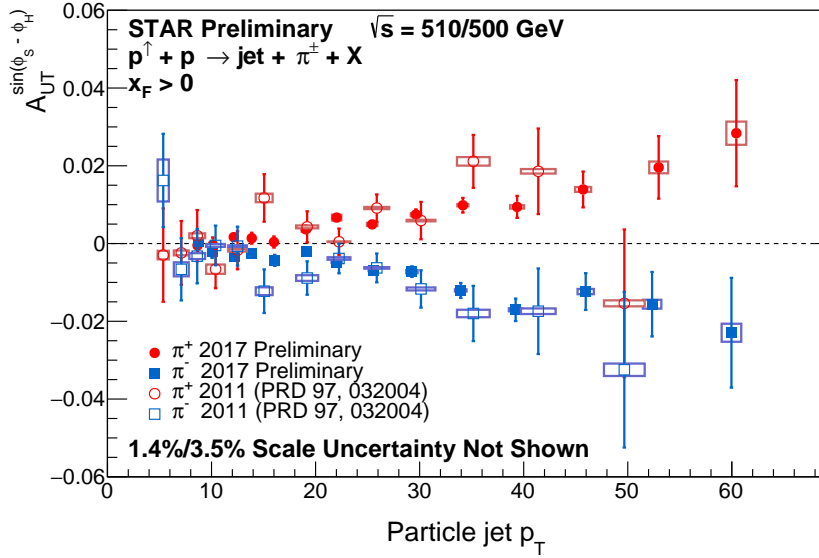


**Figure 3:** Collins asymmetries,  $A_{UT}^{\sin(\phi_S - \phi_H)}$ , for  $\pi^\pm$  in  $pp$  collisions at  $\sqrt{s} = 510/500$  GeV. The solid points show the results from this analysis at  $\sqrt{s} = 510$  GeV, while the open points show the STAR previous results at  $\sqrt{s} = 500$  GeV.

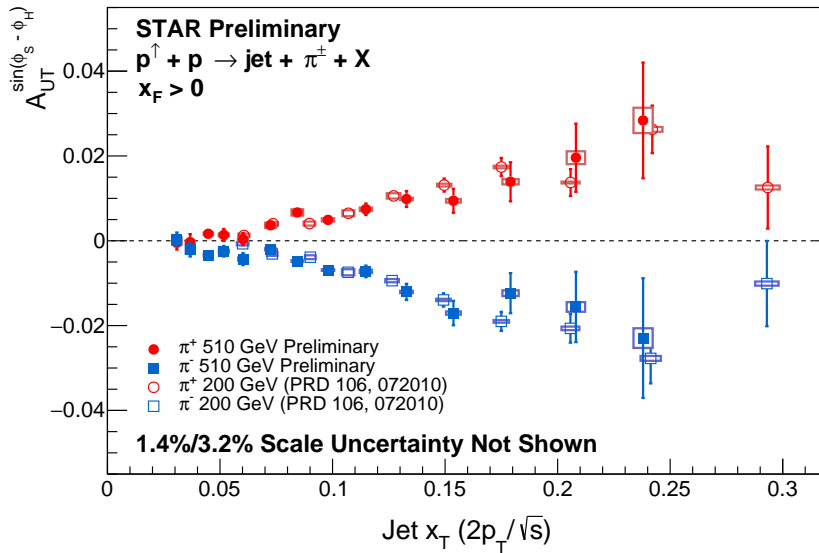


**Figure 4:** Collins asymmetries,  $A_{UT}^{\sin(\phi_S - \phi_H)}$ , as a function of particle jet  $x_T (= 2p_T/\sqrt{s})$ . The solid points show the results from this analysis of  $\sqrt{s} = 510$  GeV  $pp$  collisions, while the open points show the previous STAR results at  $\sqrt{s} = 200$  GeV [17].

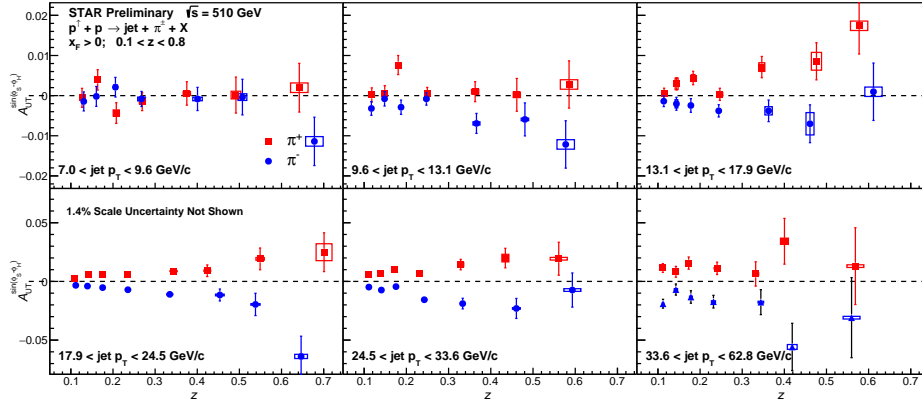


**Figure 5:**  $\pi^\pm$  Collins asymmetries,  $A_{UT}^{\sin(\phi_S - \phi_H)}$ , versus momentum fraction  $z$  in  $pp$  collisions at  $\sqrt{s} = 510$  GeV in different jet- $p_T$  bins.

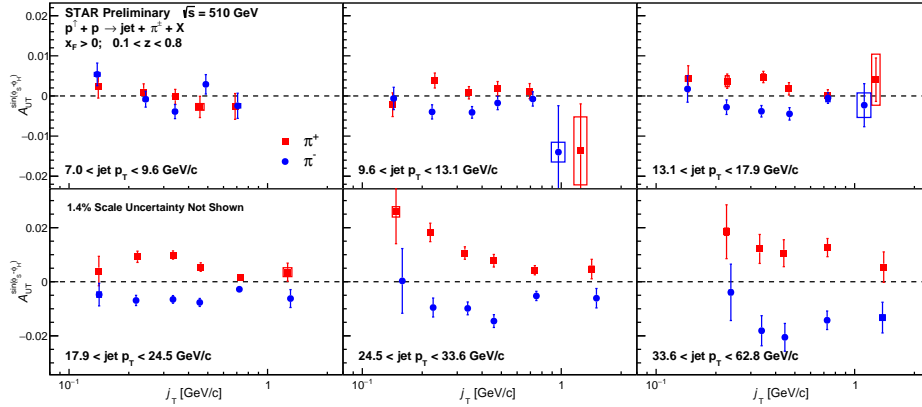


**Figure 6:**  $\pi^\pm$  Collins asymmetries,  $A_{UT}^{\sin(\phi_S - \phi_H)}$ , versus transverse momentum  $j_T$  relative to the jet axis in  $pp$  collisions at  $\sqrt{s} = 510$  GeV in different jet- $p_T$  bins.

118 510 GeV are in excellent agreement with the 200 GeV results, indicating no energy dependence.  
 119 Due to an enhancement in statistics, the Collins asymmetries for  $\pi^+$  and  $\pi^-$  versus  $z$  and  $j_T$  are  
 120 extracted. These measurements provide important constraints on the scale evolution, and a test  
 121 for the universality of the Collins asymmetry. In addition, a large data sample ( $400 \text{ pb}^{-1}$ ) with  
 122 52% polarization of transversely polarized  $pp$  collisions was recorded in 2022 by STAR, with  
 123 the forward detector ( $2.5 < \eta < 4$ ) installed, which provides a unique opportunity to study the  
 124 transverse single-spin asymmetry in the forward region.

## 125 5. Acknowledgements

126 The author is supported partially by the National Natural Science Foundation of China under  
 127 No. 12075140.

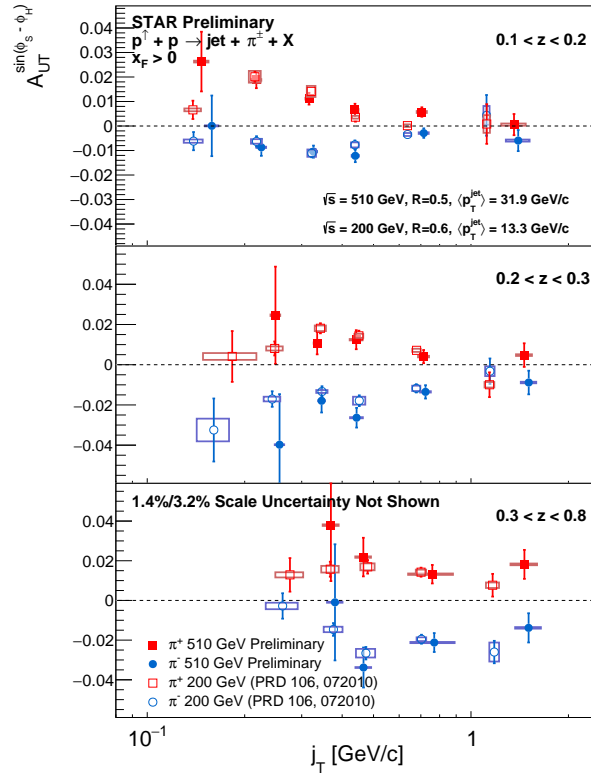


**Figure 7:** Comparison of  $\pi^\pm$  Collins asymmetries,  $A_{UT}^{\sin(\phi_S - \phi_H)}$ , between  $\sqrt{s} = 510$  GeV and  $\sqrt{s} = 200$  GeV versus transverse momentum relative to the jet axis,  $j_T$ , in different  $z$  bins.

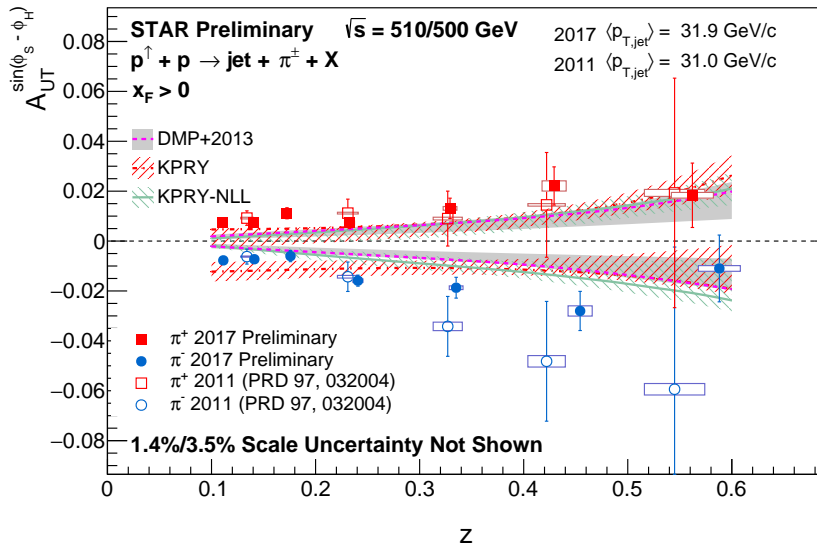


**Figure 8:** Collins asymmetries,  $A_{UT}^{\sin(\phi_S - \phi_H)}$ , as a function of charged pion's longitudinal momentum fraction,  $z$ . The asymmetries are compared with model calculations from Ref. [14, 30]



128 **References**

- 129 [1] C. A. Aidala, S. D. Bass, D. Hasch and G. K. Mallot, *Rev. Mod. Phys.* **85**, 655-691 (2013)
- 130 [2] G. L. Kane, J. Pumplin and W. Repko, *Phys. Rev. Lett.* **41**, 1689 (1978)
- 131 [3] A. V. Efremov and O. V. Teryaev, *Sov. J. Nucl. Phys.* **36**, 140 (1982)
- 132 [4] J. w. Qiu and G. F. Sterman, *Phys. Rev. Lett.* **67**, 2264-2267 (1991)
- 133 [5] D. W. Sivers, *Phys. Rev. D* **41**, 83 (1990)
- 134 [6] J. C. Collins, *Nucl. Phys. B* **396**, 161-182 (1993)
- 135 [7] A. Mukherjee and W. Vogelsang, *Phys. Rev. D* **86**, 094009 (2012)
- 136 [8] H. L. Lai, M. Guzzi, J. Huston, Z. Li, P. M. Nadolsky, J. Pumplin and C. P. Yuan, *Phys. Rev.*  
137 *D* **82**, 074024 (2010)
- 138 [9] J. Collins and J. W. Qiu, *Phys. Rev. D* **75**, 114014 (2007)
- 139 [10] T. C. Rogers and P. J. Mulders, *Phys. Rev. D* **81**, 094006 (2010)
- 140 [11] F. Yuan, *Phys. Rev. Lett.* **100**, 032003 (2008)
- 141 [12] F. Yuan, *Phys. Rev. D* **77**, 074019 (2008)
- 142 [13] Z. B. Kang, X. Liu, F. Ringer and H. Xing, *JHEP* **11**, 068 (2017)
- 143 [14] Z. B. Kang, A. Prokudin, F. Ringer and F. Yuan, *Phys. Lett. B* **774**, 635-642 (2017)
- 144 [15] L. Adamczyk *et al.* [STAR], *Phys. Rev. D* **97**, no.3, 032004 (2018)
- 145 [16] B. B. Abelev *et al.* [ALICE], *Phys. Rev. D* **91**, no.11, 112012 (2015)
- 146 [17] M. Abdallah *et al.* [STAR], *Phys. Rev. D* **106**, no.7, 072010 (2022)
- 147 [18] M. Anderson, J. Berkovitz, W. Betts, R. Bossingham, F. Bieser, R. Brown, M. Burks,  
148 M. Calderon de la Barca Sanchez, D. A. Cebra and M. G. Cherney, *et al.* *Nucl. Instrum.*  
149 *Meth. A* **499**, 659-678 (2003)
- 150 [19] W. J. Llope [STAR], *Nucl. Instrum. Meth. A* **661**, S110-S113 (2012)
- 151 [20] M. Beddo *et al.* [STAR], *Nucl. Instrum. Meth. A* **499**, 725-739 (2003)
- 152 [21] C. E. Allgower *et al.* [STAR], *Nucl. Instrum. Meth. A* **499**, 740-750 (2003)
- 153 [22] R. L. Jaffe and A. Manohar, *Phys. Lett. B* **223**, 218-224 (1989)
- 154 [23] M. Nzar and P. Hoodbhoy, *Phys. Rev. D* **45**, 2264-2268 (1992)
- 155 [24] U. D'Alesio, F. Murgia and C. Pisano, *Phys. Rev. D* **83**, 034021 (2011)

- 156 [25] G. G. Ohlsen and P. W. Keaton, Nucl. Instrum. Meth. **109**, 41-59 (1973)
- 157 [26] M. Cacciari, G. P. Salam and G. Soyez, JHEP **04**, 063 (2008)
- 158 [27] J. w. Qiu and G. F. Sterman, Phys. Rev. D **59**, 014004 (1999)
- 159 [28] L. Gamberg, Z. B. Kang and A. Prokudin, Phys. Rev. Lett. **110**, no.23, 232301 (2013)
- 160 [29] U. D'Alesio, L. Gamberg, Z. B. Kang, F. Murgia and C. Pisano, Phys. Lett. B **704**, 637-640  
161 (2011)
- 162 [30] U. D'Alesio, F. Murgia and C. Pisano, Phys. Lett. B **773**, 300-306 (2017)